Quinazolinones and Pyrido[3,4-*d*]pyrimidin-4-ones as Orally Active and Specific Matrix Metalloproteinase-13 Inhibitors for the Treatment of Osteoarthritis

Jie Jack Li,* Joe Nahra,† Adam R. Johnson, Amy Bunker, Patrick O'Brien, Wen-Song Yue, Daniel F. Ortwine, Chiu-Fai Man, Vijay Baragi, Kenneth Kilgore, Richard D. Dyer, and Hyo-Kyung Han

Department of Chemistry, Michigan Laboratories, Pfizer Global Research and Development, 2800 Plymouth Road, Ann Arbor, Michigan 48105

Received October 10, 2007

Quinazolinones **8** and pyrido[3,4-*d*]pyrimidin-4-ones **9** as orally active and specific matrix metalloproteinase-13 inhibitors were discovered for the treatment of osteoarthritis. Starting from a high-through-put screening (HTS) hit thizolopyrimidin-dione **7**, we obtained two chemotypes, **8** and **9**, using computer-aided drug design (CADD) and methodical structure–activity relationship (SAR) studies. They occupy the unique S_1'-specificity pocket and do not bind to the Zn^{2+} ion. Some pyrido[3,4-*d*]pyrimidin-4-ones, such as **10a**, possess favorable absorption, distribution, metabolism, and elimination (ADME) and safety profiles. **10a** effectively prevents cartilage damage in rabbit animal models of osteoarthritis without inducing musculoskeletal side effects when given at extremely high doses to rats.

Introduction

Gross and Lapiere discovered the first matrix metalloproteinase (MMP-1, also known as collagenase 1) from a metamorphosing tadpole in 1962.[1] Today, matrix metalloproteinases (MMPs)[a] are elucidated as a family of more than 28 subtypes of zinc- and calcium-dependent endopeptidases that are involved in the degradation of the extracellular matrix (ECM). MMPs have been implicated with many inflammatory diseases, cancers, and other illnesses.[2] Scientists in both academia and industry have carried out an enormous amount of investigations into the use of MMP inhibitors as innovative medicines.[3] Many potent and orally active broad-spectrum MMP inhibitors have been discovered and investigated in clinical trials. MMP inhibitors **1** (marimastat)[4] and **2** (prinomastat)[5] were tested against cancers; MMP inhibitors **3** (cipemastat)[6] and **4** (ilomastat)[7] were tried in the clinics for inflammation. Unfortunately, these broad-spectrum MMP inhibitors have been limited by nonspecificity and the subsequent nonselective toxicity and dose-limiting efficacy. Recognizing that the hydroxamic acid in **1**–**4** could be a possible culprit for safety issues because of its powerful chelating ability toward the MMP zinc ion, efforts have been made to replace it with milder chelating functional groups. One such group is a carboxylic acid as represented by **5** (tanomastat),[8] and another group is a thiol as represented by **6**.[9] Regrettably, there is still not a single MMP inhibitor that has emerged on the market thus far. The sole exception is probably doxycycline, which was marketed as an antibiotic but was later found to inhibit MMP-2, -8, -9, and -13.[10]

To overcome the nonselective toxicity and dose-limiting efficacy, an industry-wide effort has been undertaken to seek selective MMP inhibitors. In particular, MMP-13 has attracted much attention.[11–15] MMP-13 catalyzes the hydrolysis of type-II collagen at a unique site, which results in $^3/_4$- and $^1/_4$-length polypeptide products.[16–20] MMP-13 is not expressed in normal adult tissues, but it is found in the joints and articular cartilage of osteoarthritis (OA) patients. Therefore, it is a compelling target for the treatment of OA.[21–25] An MMP-13 inhibitor has been shown to block the degradation of explanted human osteoarthritic cartilage.[19] In genetically modified mice, regulated expression of human MMP-13 induces osteoarthritis.[26] On the basis of these findings, it is likely that MMP-13 causes irreversible cartilage damage in OA, and therefore, a selective MMP-13 inhibitor would effectively prevent cartilage degradation without causing musculoskeletal syndrome (MSS) side effects that have plagued many MMP broad-spectrum inhibitors in clinical development.[24,26,27]

Scheme 1. Synthesis of Alkynyl Quinazolinones **8**

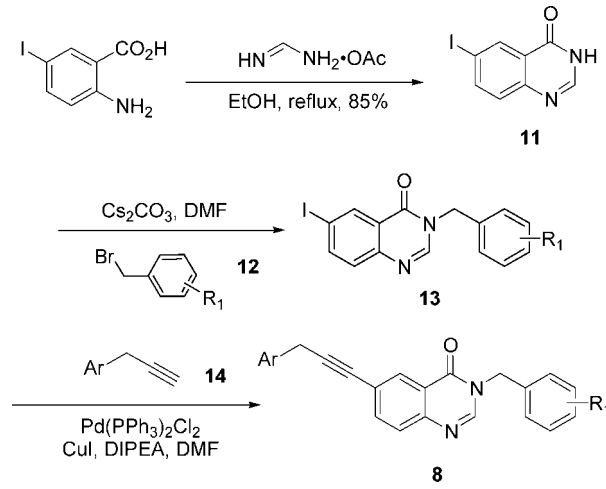

High-through-put screening (HTS) of our compound collection provided, in addition to all of the broad-spectrum MMP inhibitors, a unique hit, thiazolopyrimidinedione **7**, which possessed an astounding selectivity for MMP-13 versus other MMP isoforms (Figure 2). As a matter of fact, it was *specific* for MMP-13 for all practical purposes. Cocrystallization of **7** with the MMP13-CD (catalytic domain) revealed an unexpected nonzinc-binding mode: instead of binding to the Zn^{2+} cation,

* To whom correspondence should be addressed: Discovery Chemistry, Bristol-Myers Squibb Company, 5 Research Parkway, Wallingford, CT 06492. Telephone: (203) 677-7255. E-mail: jie.li1@bms.com.

† Present address: Discovery Chemistry, Bristol-Myers Squibb Company, P.O. Box 5400, Princeton, NJ 08543-5400.

[a] Abbreviations: ADME, absorption, distribution, metabolism, and elimination; AUC, area under curve; CADD, computer-aided drug design; CD, catalytic domain; CIR, confidence in rationale; ECM, extracellular matrix; HTS, high-through-put screening; IVMN, *in vitro* micronucleus; MMP, matrix metalloproteinase; MSS, musculoskeletal syndrome; OA, osteoarthritis; SAR, structure–activity relationship.

10.1021/jm701274v CCC: $40.75
Published on Web 02/06/2008

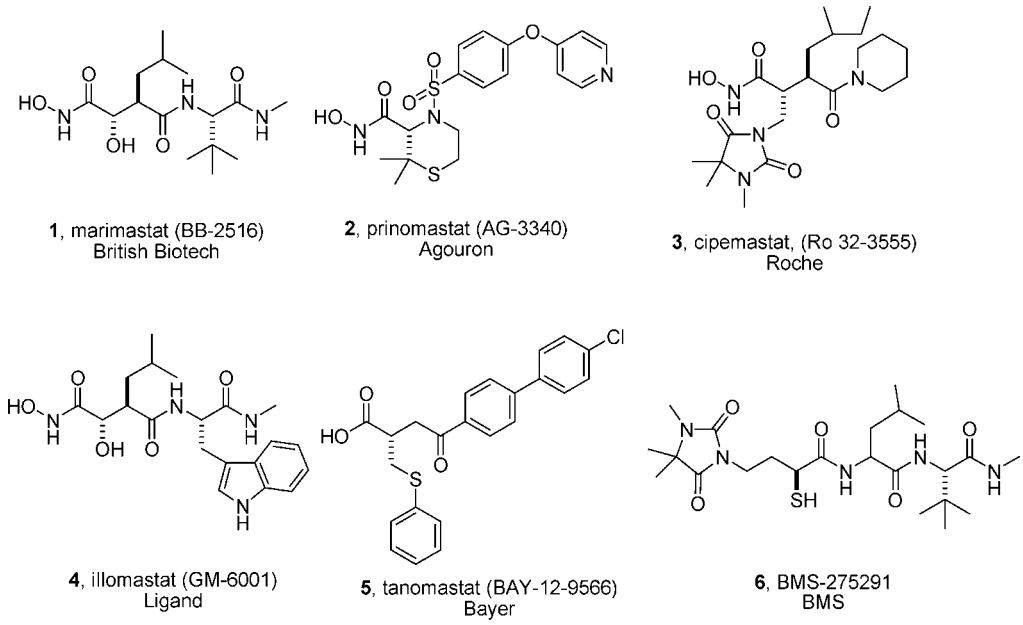

Figure 1. Broad-spectrum MMP inhibitors.

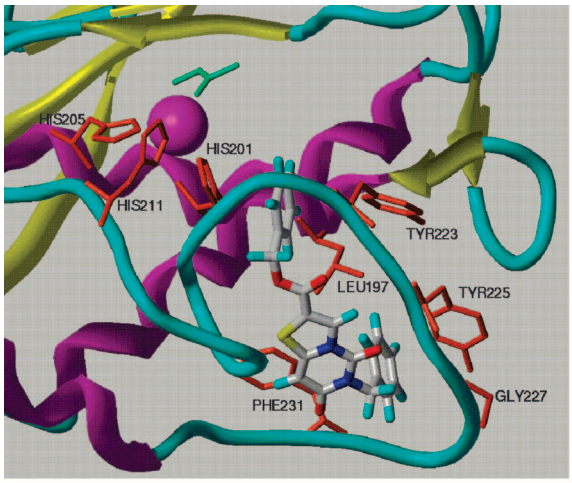

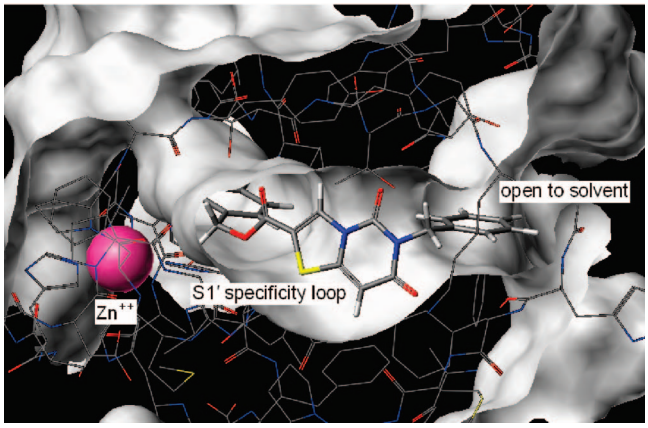

Figure 2. Nonzinc-binding mode of **7** from the cocrystal structure (1.72 Å) with the MMP-13 catalytic domain enzyme, with **7** occupying the S_1'-specificity pocket.

1 binds deep within the S_1'-specificity loop of the protein and extends past this pocket out toward the bulk solvent (Figure 2). In describing the specificity of peptidases, S_1 is the first specificity subunit from the catalytic site (Zn^{2+} in this case)

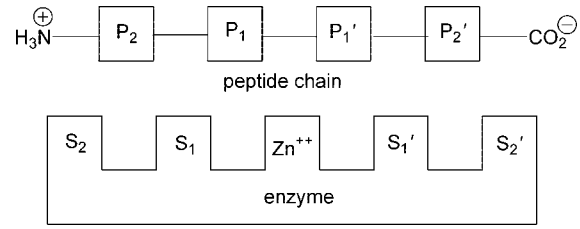

Figure 3. Definition of the specificity loops of peptidases.

toward the N terminus and S_1' is the first specificity subunit from the catalytic site toward the C terminus (Figure 3). The MMP catalytic domain consists of a five-stranded β-sheet and a 3-α-helices, with the catalytic site defined by β-strand IV and the central helix, which imparts significant structural differences for MMP isoforms. The S_1'-specificity pocket in MMP-13 is an unusually large, open channel, nearly twice the size as that found in MMP-1, which may explain the high degree of specificity of **7**.

However, **7** is an ester, metabolizing readily in the body, and the corresponding acid is inactive in MMP-binding assays. Using computer-aided drug design (CADD) and methodical structure–activity relationship (SAR) studies, we obtained two series, quinazolinones **8** and **9** and pyrido[3,4-*d*]pyrimidin-4-ones **10** (Figure 4), that are potent and specific MMP-13 inhibitors, some of which are orally bioavailable. These specific MMP-13 inhibitors, occupying the unique S_1'-specificity pocket, do not bind to the Zn^{2+} ion, effectively preventing cartilage damage in animal models of osteoarthritis without inducing musculoskeletal side effects when given at extremely high doses to rats.

Results and Discussion

Chemistry. Synthesis of alkynyl quinazolinones **8** began with condensation of commercially available 2-amino-5-iodo-benzoic acid with formamidine acetate in refluxing ethanol to afford 6-iodo-3*H*-quinazolin-4-one (**11**).[28,29] The key intermediate **11** enabled convenient SAR investigation at both 3 and 6 positions. Therefore, alkylation of **11** with benzyl chloride **12** in the presence of Cs_2CO_3 gave rise to the 3-*N*-benzylated products **13**. Finally, a Sonogashira reaction between **13** and 3-phenyl-1-propyne **14** delivered alkynyl quinazolinones **8** (Scheme 1).

Scheme 2. Synthesis of Amide Quinazolinones **9**

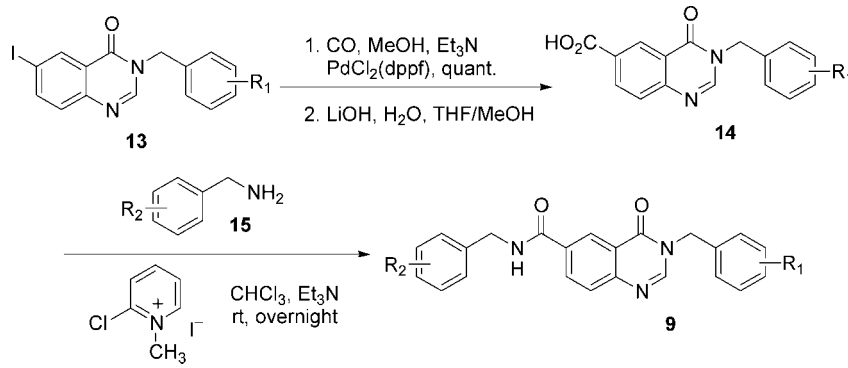

Synthesis of the amide quinazolinones **9** was similar to that of the alkynyl quinazolinones **8** (Scheme 2). Instead of a Sonogashira coupling reaction, a palladium-catalyzed carbonylation of **13** was followed by hydrolysis to produce carboxylic acid **14**. A Mukaiyama amide formation with benzylamine **15** then delivered the desired amide quinazolinones **9**.

To block the metabolism site at the C-7 position, efforts were made to replace the C−H with a nitrogen atom as amide pyrido[3,4-*d*]pyrimidin-4-ones **10**. Therefore, adduct **17** was produced from alkylation of the known chloropyrido[3,4-*d*]pyrimidin-4(3*H*)-one (**16**)[29] with benzyl bromide **12**. Palladium-catalyzed carbonylation of **17** afforded methyl ester **18**. After Weinreb's one-step amidation protocol,[30–32] ester **18** was

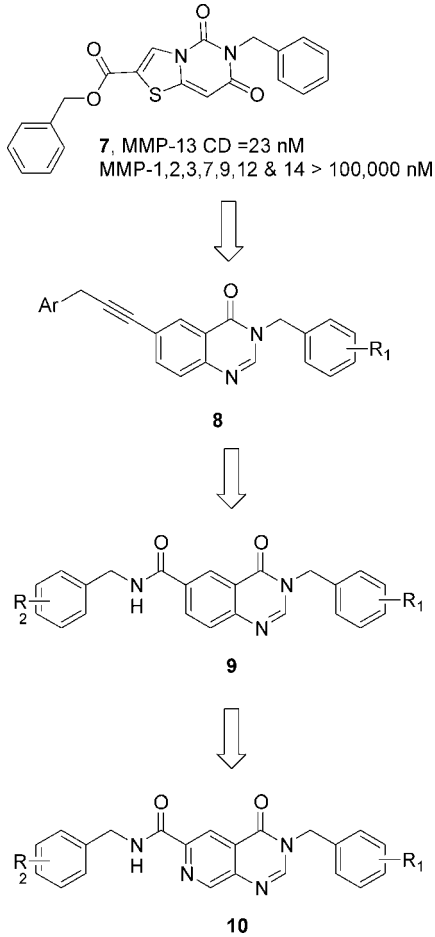

Figure 4. Progression of the SAR: from thiazolopyrimidinedione **7** to quinazolinones **8** and **9** and to pyrido[3,4-*d*]pyrimidin-4-ones **10**.

Scheme 3. Synthesis of Amides Pyrido[3,4-*d*]pyrimidin-4-ones **10**

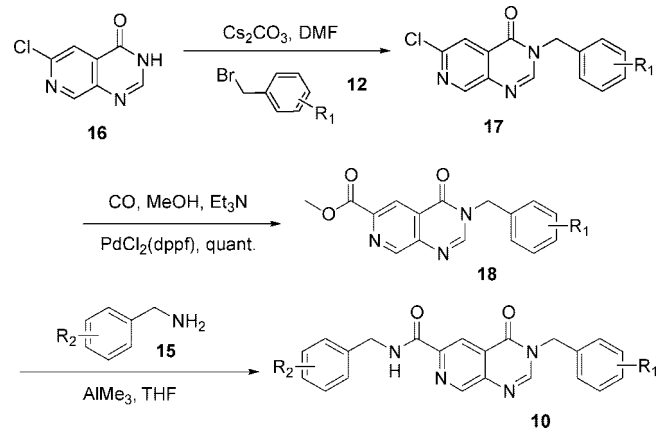

then treated with the dimethylaluminum amide generated from $AlMe_3$ and benzylamine **15** to deliver the final amides **10** (Scheme 3).

Structural−Activity Relationship. When the synthetic route delineated in Scheme 1 was applied, a series of alkynyl quinazalinones were synthesized with variations at both the solvent end and the S1′-specificity pocket. For the solvent end, as shown in entries 1–10, tetrazole **8a** and carboxylic acid **8b** were the most potent substituents for the binding of both catalytic domain (CD) and full-length collagen.[33] The potency was eroded somewhat for other less acidic analogues, such as 2,6-diflurophenol **8c**, carboxamide **8d**, and sulfonamide **8e**. For derivatives without an acidic moiety (entries 6–9, **8f–8i**), the potency suffered even further. In all, the potency is closely associated with the pK_a of the fragment aligned in the solvent cavity (thereby the hydrogen-bond-donating ability).

Because carboxylic acid provided the best potency, the solvent end was kept constant as a carboxylic acid in the process of investigating the SAR of the S1′-specificity pocket. The nature of the substituent of the compound binding to the S1′-specificity pocket has a significant impact on the potency as well. For instance, when the S1′-specificity pocket was occupied by an aromatic ring, such as entry 2 (Table 1), compound **8b** was very potent (IC_{50} = 1.54 nM). However, the corresponding allene analogue **8k** (entry 11) was over 100-fold less potent (IC_{50} = 194 nM) possibly because its steric alignment did not fit in the S1′-specificity pocket as well. The two aliphatic cyclic amine derivatives **8l** and **8m** fit in the binding pocket tightly, implying the importance of the π-stacking in achieving binding potency. Indeed, heteroaryl substituent at the S1′-specificity pocket, such as imidazole, restored the potency as demonstrated

Table 1. SAR of Alkynyl Quinazalinones **8** for the Solvent End (Entries 1–9) and the S1′ End (Entries 10–14)

Entry	Comp ID	Structure	MMP-13 CD av. IC_{50} (nM)[a]	Collagen II av. IC_{50} (nM)[b]
1	**8a**	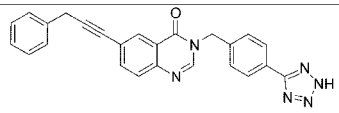	0.88	6.5
2	**8b**	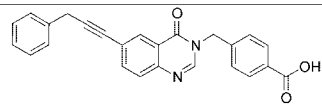	1.54	9.8
3	**8c**	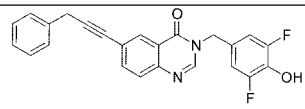	6.12	18.0
4	**8d**	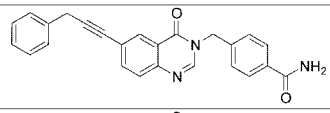	13.5	140
5	**8e**	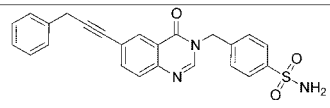	13.9	79
6	**8f**	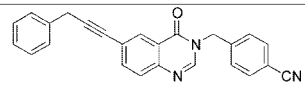	36.3	122
7	**8g**	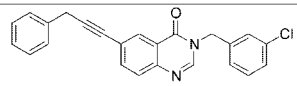	61.2	610
8	**8h**	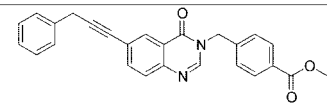	63.2	244
9	**8i**	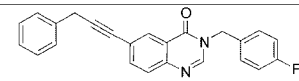	130	
10	**8j**	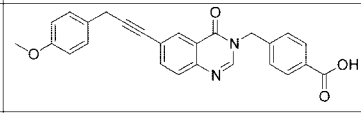	0.15	0.78
11	**8k**	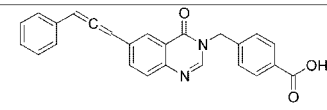	194	100,000
12	**8l**	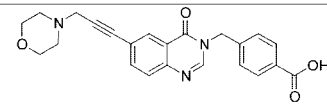	65,000	100,000
13	**8m**	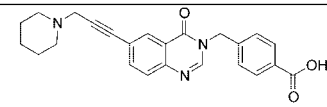	75,000	100,000
14	**8n**	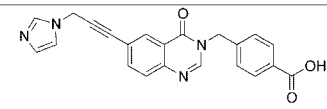	7.82	57

[a] "MMP-13 CD av. IC_{50} (nM)" represents the average IC_{50} value in nanomolars for the binding assay of the compound using the MMP-13 catalytic domain enzyme. [b] "MMP-13 Collagen II av. IC_{50} (nM)" represents the average IC_{50} value in nanomolars for the binding assay of the compound using the MMP-13 full-length enzyme.

in entry 14 (IC_{50} = 7.82 nM for **8n**). **8n** has an added benefit of increased aqueous solubility.

While the alkynyl quinazalinones **8** furnished great potency and bioavailability, our *in vitro* adduct formation studies indicated potential safety issues. Moreover, the ease of isomerization of benzyl alkynes to the corresponding allenes (e.g., **8b** → **8k**) under basic conditions added further concerns regarding the chemical stability of these compounds. In the literature, some acetylene-containing drugs (e.g., efavirenz) were extensively metabolized *in vivo* from cytochrome P450 interactions and the activation of the alkyne led to a cysteinylglycine adduct.[34] As a consequence, nephrotoxicity was observed for efavirenz. Although the mere presence of an alkyne in a molecule is not sufficient to produce nephrotoxic events from cytochrome P450 interactions, a decision was made to pursue amide as a bioisostere for the ester instead of the alkyne as in alkynyl quinazalinones **8** to avoid further complications.

The synthesis was achieved using chemistry delineated in Scheme 2, and the SAR of amide quinazalinones **9** is shown in Table 2 (entries 1–4). Similar to the SAR of **8**, carboxylic acid at the solvent end afforded the highest potency (hydroxamic acid was intentionally avoided because of selectivity concerns). In agreement with our docking (onto the MMP-13 CD enzyme) and overlay studies, the amide quinazolinones **9** are found to be generally less potent than the corresponding alkynyl quinazolinones **8**. The most potent amide analogue **9a** is 10-fold less potent than the corresponding alkyne analogue **8j**.

Because CYP450 oxidation of **9** was the major metabolism pathway to give the corresponding phenol at the C-7 position of the amide quinazolinones, efforts were made to block the position by making pyrido[3,4-*d*]pyrimidin-4-ones **10** with amides at the S1′ end. The SAR trends of amide pyrido[3,4-*d*]pyrimidin-4-ones **10** bear a striking resemblance to the corresponding amide quinazolinones **9**, although **10** is generally less potent than **9**.[35–37] For instance, carboxylic acid **10a**, with an IC_{50} of 6.72 nM, is about 4-fold less potent than the corresponding carboxylic acid **9a**, with an IC_{50} of 1.61 nM.

Pharmacokinetics, Safety, and Efficacy. We further investigated the absorption, distribution, metabolism, and elimination (ADME) profiles for MMP-13 inhibitors with IC_{50} < 10 nM in the binding assay using truncated enzyme containing the catalytic domain and IC_{50} < 100 nM in the binding assay using the full-length enzyme. Some exceptions to these *in vitro* profile cut-offs were made for representative chemotypes to understand the correlation between structure and bioavailability. Some of the alkynyl quinazalinones **8** tested gave favorable oral bioavailability. For instance, carboxylic acid **8b** with 3-phenyl-1-propyne moiety at the S1′ end has moderate clearance and moderate volume distribution in rats as shown in Table 3 (entry 1). As a result, **8b** has a half-life of 5.4 h, *F*% of 75%, and area under curve (AUC) of 12 400 ng h^{-1} mL^{-1} (po). The corresponding methoxyl analogue **8j** has a similar, although slightly less favorable, pharmacokinetics profile than that of **8b**. These alkynes were not further pursued because of safety concerns (*vide supra*). As far as amide quinazalinones **9** were concerned, none of the derivatives in this series possessed desirable oral bioavailability in rats, as exemplified by amides **9a** and **9b** in entries 5 and 6 in Table 3. It was found that oxidative metabolism of amides **9a** and **9b** took place on the benzene ring of the quinazalinone core structure. In an effort to block

Table 2. SAR of Amide Quinazalinones **9** and Amide Pyrido[3,4-*d*]pyrimidin-4-ones **10**

Entry	Comp ID	Structure	MMP-13 CD av. IC50 (nM)[a]	Collagen II av. IC50 (nM)[b]
1	**9a**	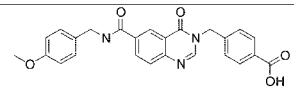	1.61	11.0
2	**9b**	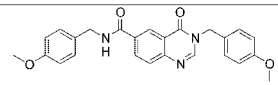	365	6,000
3	**9c**	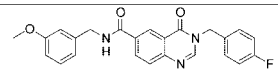	237	3,000
4	**9d**	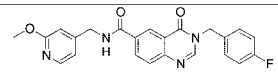	728	10,000
5	**10a**	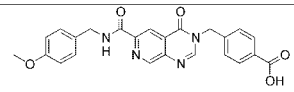	6.72	30.5
6	**10b**	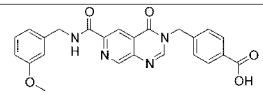	13.8	120
7	**10c**	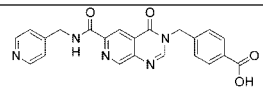	49.4	184
8	**10d**	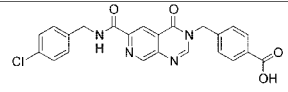	9.95	28.0
9	**10e**	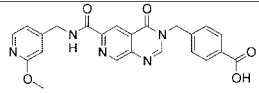	3.46	18.0
10	**10f**	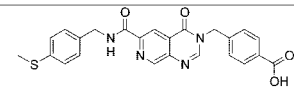	11.0	48.0
11	**10g**	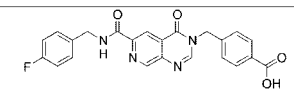	4.24	37.0
12	**10h**	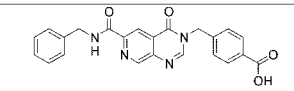	19.3	120.0
13	**10i**	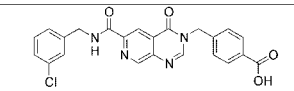	2.69	21.2
14	**10j**	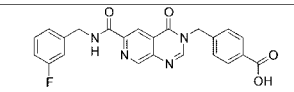	16.4	46.0
15	**10k**	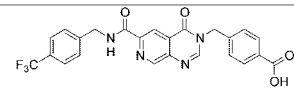	95.6	1,900
16	**10l**	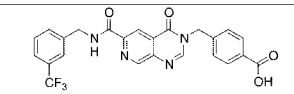	25.3	184
17	**19a**	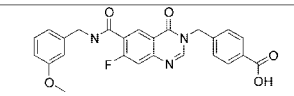	31.1	1,710

[a] "MMP-13 CD av. IC_{50} (nM)" represents the average IC_{50} value in nanomolars for the binding assay of the compound using the MMP-13 catalytic domain enzyme. [b] "MMP-13 Collagen II av. IC_{50} (nM)" represents the average IC_{50} value in nanomolars for the binding assay of the compound using the MMP-13 full-length enzyme.

Table 3. Pharmacokinetics Data for Selected MMP-13 Inhibitors

entry	compound	CL (mL min^{-1} kg^{-1})	Vdss (L/kg)	AUC ($0 \rightarrow \infty$) (ng h^{-1} mL^{-1}) (po)	$T_{1/2}$ (h)	*F*%	solubility (μg/mL)
1	**8b**	4.9	0.6	12 400	5.4	75	3
2	**8c**	39.4	2.8	41	0.7	2	<3
3	**8j**	5.3	1	5160		40	4.5
4	**8n**	31	1.9	570	0.9	19	>60
5	**9a**	20.0	0.4	377	3.5	9	89.6
6	**9b**	23.5	1.5	1720	1.4	48	1
7	**10a**	7.6	0.9	13 400	3.9	73	60
8	**10b**	11.2	0.5	1810	2.3	24	60
9	**10l**	20.6	2	1010			
10	**19a**	16.4	0.5	1470	2.1	40	41

this oxidation, a fluorine was installed at the C-7 position to give **19a**. Regrettably, not only was it less potent with an IC_{50} of 31.1 nM in the MMP-13 CD assay (entry 18 in Table 2), **19a** also had low oral bioavailability in rats (entry 10 in Table 3). Gratifyingly, when the C−H moiety was replaced with a nitrogen atom, amide pyrido[3,4-*d*]pyrimidin-4-ones **10** had both an increase in potency and an increase in solubility, as well as elevated bioavailability in some cases. Moreover, **10a** has a moderate clearance and moderate volume distribution in rats as shown in Table 3 (entry 7). As a result, its half-life is 3.9 h, *F*% of 73%, and AUC (po) of 13400 ng h^{-1} mL^{-1}.

Because of the favorable ADME profile of **10a**, it was further characterized more thoroughly. It is a potent MMP-13 inhibitor with an IC_{50} of 6.72 nM in the MMP-13 CD assay but does not inhibit all other MMP isozymes tested, including MMP-1, MMP-2, MMP-3CD, MMP-7, MMP-8CD, MMP-9, MMP-12, MMP-14CD, and MMP-17CD. Possibly thanks to its remarkable specificity, similar to the outcome of the vehicle, no undesirable MSS was observed for **10a**, while a broad-spectrum MMP inhibitor caused MSS for 12 out of 12 rats treated with it. Therefore, in the rat model, the MMP-13-specific inhibitor **10a** is completed devoid of MSS, a side effect that has plagued the majority of broad-spectrum MMP inhibitors in the clinics. Compound **10a** also tested negative in both mini-Ames and *in vitro* micronucleus (IVMN) tests. Furthermore, the *in vivo* toxicity study involving two species (rat and rabbit) did not show any noticeable toxicity issues (Table 4).

More significantly, a cartilage protection *in vivo* study was carried out using the NZW male rabbits that were inflicted with OA surgically. On day 35, gross morphology (lesion area and severity) indicated that, at 10 mg/kg dose, **10a** inhibited the degeneration both of tibial plateau and femoral condyle cartilage

Table 4. Rat MSS Model for Broad-Spectrum MMP Inhibitor and **10a**, $n = 12$ Sprague–Dawley Rats/Group (6 per Sex)

	Vehicle	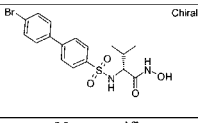	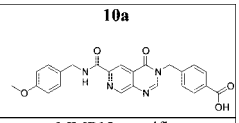
Inhibitor type	-	Non-specific	MMP13-specific
Dose (mpk/d)	-	2,000	2,000
Day 14 AUC0-24 (mg•hr/mL)	-	94 (parent) 684 (-COOH)	1,010
Rats with MSS-like joint fibroplasias	0 of 12	12 of 12	0 of 12

lesions (Figure 4).[38] The *in vivo* efficacy study in rabbits provided greater confidence in rationale (CIR) for this approach of using MMP-13-specific inhibitors to treat OA.

Conclusion

In summary, the HTS hit thiazolopyrimidinedione **7** is a MMP-13-specific inhibitor, which imparts its specificity by binding the unique S1′-specificity pocket. Our extensive SAR investigation resulted in amide pyrido[3,4-*d*]pyrimidin-4-ones **10** as MMP-13-selective inhibitors (specific versus other MMPs) that bind to the unique S_1'-specificity pocket and do not bind to the Zn^{2+} ion. Some derivatives, such as **10a**, possess favorable ADME and safety profiles. More significantly, our positive cartilage protection *in vivo* study in rabbits using **10a** provided increased CIR for this approach of using MMP-13-specific inhibitors to treat OA.

Supporting Information Available: ^{1}H NMR spectra and data and MS(APCI) data of all products and melting points and CHN elemental analysis data for all solid samples. This material is available free of charge via the Internet at http://pubs.acs.org.

References

(1) Gross, J.; Lapiere, C. Collagenolytic activity in amphibian tissues: A tissue culture assay. *Proc. Natl. Acad. Sci. U.S.A.* **1962**, *48*, 1014–1022.

(2) Stamenkovic, I. Extracellular matrix remodelling: The role of matrix metalloproteinases. *J. Pathol.* **2003**, *200*, 448–464.

(3) Skiles, J. W.; Gonnella, N. C.; Arco, Y.; Jeng, A. Y. The design, structure, and clinical update of small molecular weight matrix metalloproteinase inhibitors. *Curr. Med. Chem.* **2004**, *11*, 2911–2977.

(4) Rosenbaum, E.; Zahurak, M.; Sinibaldi, V.; Carducci, M. A.; Pili, R.; Laufer, M.; DeWeese, T. L.; Eisenberger, M. A. Marimastat in the treatment of patients with biochemically relapsed prostate cancer: A prospective randomized, double-blind, phase I/II trial. *Clin. Cancer Res.* **2005**, *11*, 4437–4443.

(5) Bissett, D.; O'Byrne, K. J.; von Pawel, J.; Gatzemeier, U.; Price, A.; Nicolson, M.; Mercier, R.; Mazabel, E.; Penning, C.; Zhang, M. H.; Collier, M. A.; Shepherd, F. A. Phase III study of matrix metalloproteinase inhibitor prinomastat in non-small-cell lung cancer. *J. Clin. Oncol.* **2005**, *23*, 842–849.

(6) Hemmings, F. J.; Farhan, M.; Rowland, J.; Banken, L.; Jain, R. Tolerability and pharmacokinetics of the collagenase-selective inhibitor Trocade in patients with rheumatoid arthritis. *Rheumatology* **2001**, *40*, 537–543.

(7) Beckett, R. P. Recent advances in the field of matrix metalloproteinase inhibitors. *Expert Opin. Ther. Pat.* **1996**, *6*, 1305–1315.

(8) Molina, J. R.; Reid, J. M.; Erlichman, C.; Sloan, J. A.; Furth, A.; Safgren, S. L.; Lathia, C. D.; Alberts, S. R. A phase I and pharmacokinetic study of the selective, non-peptidic inhibitor of matrix metalloproteinase BAY 12-9566 in combination with etoposide and carboplatin. *Anti-Cancer Drugs* **2005**, *16*, 997–1002.

(9) Douillard, J.-Y.; Peschel, C.; Shepherd, F.; Paz-Ares, L.; Arnold, A.; Davis, M.; Tonato, M.; Smylie, M.; Tu, D.; Voi, M.; Humphrey, J.; Ottaway, J.; Young, K.; Vreckem, A. V.; Seymour, L. Randomized phase II feasibility study of combining the matrix metalloproteinase inhibitor BMS-275291 with paclitaxel plus carboplatin in advanced non-small cell lung cancer. *Lung Cancer* **2004**, *46*, 361–368.

(10) Hanemaaijer, R.; Visser, H.; Koolwijk, P.; Sorsa, T.; Salo, T.; Golub, L. M.; van Hinsbergh, V. W. Inhibition of MMP synthesis by doxycycline and chemically modified tetracyclines (CMTs) in human endothelial cells. *Adv. Dent. Res.* **1998**, *12*, 114–118.

(11) Tardif, G.; Reboul, P.; Pelletier, J.-P.; Martel-Pelletier, J. Ten years in the life of an enzyme: The story of the human MMP-13 (collagenase-3). *Mod. Rheumatol.* **2004**, *14*, 197–204.

(12) MMP-13 inhibitors. *Expert Opin. The. Pat.* **2005**, *15*, 237–241.

(13) Hu, Y.; Xiang, J. S.; DiGrandi, M. J.; Du, X.; Ipek, M.; Laakso, L. M.; Li, J.; Li, W.; Rush, T. S.; Schmid, J.; Skotnicki, J. S.; Tam, S.; Thomason, J. R.; Wang, Q.; Levin, J. I. Potent, selective, and orally bioavailable matrix metalloproteinase-13 inhibitors for the treatment of osteoarthritis. *Bioorg. Med. Chem.* **2005**, *13*, 6629–6644.

(14) Engel, C. K.; Pirard, B.; Schimanski, S.; Kirsch, R.; Habermann, J.; Klingler, O.; Schlotte, V.; Weithmann, K. U.; Wendt, K. U. Structural basis for the highly selective inhibition of MMP-13. *Chem. Biol.* **2005**, *12*, 181–189.

(15) Kim, S.-H.; Pudzianowski, A. T.; Leavitt, K. J.; Barbosa, J.; McDonnell, P. A.; Metzler, W. J.; Rankin, B. M.; Liu, R.; Vaccaro, W.; Pitts, W. Structure-based design of potent and selective inhibitors of collagenase-3 (MMP-13). *Bioorg. Med. Chem. Lett.* **2005**, *15*, 1101–1106.

(16) Knäuper, V.; López-Otin, C.; Smith, B.; Knight, G.; Murphy, G. Biochemical characterization of human collagenase-3. *J. Biol. Chem.* **1996**, *271*, 1544–1550.

(17) Welgus, H. G.; Kobayashi, D. K.; Jeffrey, J. J. The collagen substrate specificity of rat uterus collagenase. *J. Biol. Chem.* **1983**, *258*, 14162–14165.

(18) Mitchell, P. G.; Magna, H. A.; Reeves, L. M.; Lopresti-Morrow, L. L.; Yocum, S. A.; Rosner, P. J.; Geoghegan, K. F.; Hambor, J. E. Cloning, expression, and type II collagenolytic activity of matrix metalloproteinase-13 from human osteoarthritic cartilage. *J. Clin. Invest.* **1996**, *97*, 761–768.

(19) Billinghurst, R. C.; Dahlberg, L; Ionescu, M.; Reiner, A.; Bourne, R.; Rorabeck, C.; Mitchell, P.; Hambor, J.; Diekmann, O.; Tschesche, H.; Chen, J.; van Wart, H.; Poole, A. R. Enhanced cleavage of type II collagen by collagenases in osteoarthritic articular cartilage. *J. Clin. Invest.* **1997**, *99*, 1534–1545.

(20) Reboul, P.; Pelletier, J.-P.; Tardif, G.; Cloutier, J.-M.; Martel-Pelletier, J. The new collagenase, collagenase-3, is expressed and synthesized by human chondrocytes but not by synoviocytes: A role in osteoarthritis. *J. Clin. Invest.* **1996**, *97*, 2011–2019.

(21) Wernicke, D.; Seyfert, C.; Hinzmann, B.; Gromnica-Ihle, E. Cloning of collagenase 3 from the synovial membrane and its expression in rheumatoid arthritis and osteoarthritis. *J. Rheumatol.* **1996**, *23*, 590–595.

(22) Freemont, A. J.; Byers, R. J.; Taiwo, Y. O.; Hoyland, J. A. *In situ* zymographic localization of type II collagen degrading activity in osteoarthritic human articular cartilage. *Ann. Rheum. Dis.* **1999**, *58*, 357–365.

(23) Neuhold, L. A.; Killar, L.; Zhao, W.; Sung, M.-L. A.; Warner, L.; Kulik, J.; Turner, J.; Wu, W.; Billinghurst, C.; Meijers, T.; Robin Poole, A.; Babij, P.; DeGennaro, L. J. Postnatal expression in hyaline cartilage of constitutively active human collagenase-3 (MMP13) induces osteoarthritis in mice. *J. Clin. Invest.* **2001**, *107*, 35–44.

(24) Clark, I. M.; Parker, A. E. Metalloproteinases: Their role in arthritis and potential as therapeutic targets. *Exp. Opin. Ther. Targets* **2003**, *7*, 19–34.

(25) Drummond, A. H.; Beckett, P.; Brown, P. D.; Bone, E. A.; Davidson, A. H.; Galloway, W. A.; Gearing, A. J.; Huxley, P.; Laber, D.; McCourt, M.; Whittaker, M.; Wood, L. M.; Wright, A. Preclinical and clinical studies of MMP inhibitors in cancer. *Ann. N.Y. Acad. Sci.* **1999**, *878*, 228–235.

(26) Renkiewicz, R.; Qiu, L.; Lesch, C.; Sun, X.; Devalaraja, R.; Cody, T.; Kaldjian, E.; Welgus, H.; Baragi, V. Broad-spectrum matrix metalloproteinase inhibitor marimastat-induced musculoskeletal side effects in rats. *Arthritis Rheum.* **2003**, *48*, 1742–1749.

(27) Schechter, I.; Berger, A. On the size of the active site in proteases. *Biochem. Biophys. Res. Commun.* **1967**, *27*, 157–162.

(28) Stevenson, T. M.; Kazmierczak, F.; Leonard, N. J. Defined dimensional alterations in enzyme substrates. General synthetic methodology for the bent dihydro-lin-benzopurines. *J. Org. Chem.* **1986**, *51*, 616–621.

(29) Rewcastle, G. W.; Denny, W. A.; Winters, R. T.; Colbry, N. L.; Showalter, H. D. H. Synthesis of 6-substituted pyrido[3,4-*d*]pyrimidin-4-ones via directed lithiation of 2-substituted 5-aminopyridine derivatives. *J. Chem. Soc., Perkin Trans.* **1996**, *1*, 2221–2226.

(30) Basha, A.; Lipton, M.; Weinreb, S. W. A mild, general method for conversion of esters to amides. *Tetrahedron Lett.* **1977**, *48*, 4171–4174.

(31) Levin, J. I.; Turos, E.; Weinreb, S. W. An alternative procedure for the aluminum-mediated conversion of esters to amides. *Synth. Commun.* **1982**, *12*, 989–993.

(32) For a review, see Montalbettis, C. A. G. N.; Falque, V. Amide bond formation and peptide coupling. *Tetrahedron* **2005**, *61*, 10827–10852.

(33) Biology: For catalytic domain MMP-13 binding, MMP-13A, MMP-13 TPL HUM pH 7 NO BRIJ. For full-length MMP-13 binding, MMP-13E, MMP-13 FL HUM pH 7 NO BRIJ. Thiopeptolide substrates show virtually no decomposition or hydrolysis at or below neutral pH in the absence of a matrix metalloproteinase enzyme. A typical thiopeptolide substrate commonly used for assays is Ac-Pro-Leu-Gly-thioester-Leu-Leu-Gly-OEt. A 100 μL assay mixture will contain 50 mM of *N*-2-hydroxyethylpiperazine-*N*-2-ethanesulfonic acid buffer ("HEPES" at pH 7.0), 10 mM $CaCl_2$, 100 μM thiopeptolide substrate, and 1 mM 5,5′-dithio-bis-(2-nitro-benzoic acid) (DTNB). The thiopeptolide substrate concentration may be varied, for example, from 10 to 800 μM to obtain K_m and K_{cat} values. The change in absorbance at 405 nm is monitored on a Thermo Max microplate reader (Molecular Devices, Menlo Park, CA) at room temperature (22 °C). The calculation of the amount of hydrolysis of the thiopeptolide substrate is based on $E_{412} = 13\,600\ M^{-1}\ cm^{-1}$ for the DTNB-derived product 3-carboxy-4-nitrothiophenoxide. Assays are carried out with and without matrix metalloproteinase inhibitor compounds, and the amount of hydrolysis is compared for a determination of inhibitory activity of the test compounds. Test compounds were evaluated at various concentrations to determine their respective IC_{50} values, the micromolar concentration of compound required to cause a 50% inhibition of catalytic activity of the respective enzyme. It should be appreciated that the assay buffer used with MMP-3CD was 50 mM *N*-morpholinoethane sulfonate ("MES") at pH 6.0 rather than the HEPES buffer at pH 7.0 described above.

(34) Mutlib, A. E.; Chen, H.; Nemeth, G. A.; Markwalder, J. A.; Seitz, S. P.; Gan, L. S.; Christ, D. D. Identification and characterization of efavirenz metabolites by liquid chromatography/mass spectrometry and high field NMR: Species differences in the metabolism of efavirenz. *Drug Metab. Depos.* **1999**, *27*, 1319–1333.

(35) Gaudilliere, B.; Jacobelli, H.; Kostlan, C.; Li, J. J.; Yue, W.-s. Preparation of oxo azabicyclic compounds such as pyridopyrimidinones and quinazolinones as inhibitors of type-13 matrix metalloprotease. US2003220355, 2003.

(36) Bunker, A. M.; Picard, J. A. Azaisoquinoline derivatives as matrix metalloproteinase inhibitors, pharmaceutical compositions, and therapeutic use. WO 2004014866, 2004.

(37) Bunker, A. M.; Picard, J. A.; Lodaya, R. M.; Waldo, M. L.; Marlatt, M. E. Preparation of pyrido[3,4-*d*]pyrimidine derivatives as matrix metalloproteinase-13 inhibitors. WO2005016926, 2006.

(38) Johnson, A. R.; Pavlovsky, A. G.; Ortwine, D. F.; Prior, F.; Man, C.-F.; Bornemeier, D. A.; Banotai, C. A.; Mueller, W. T.; McConnell, P.; Yan, C.; Baragi, V.; Lesch, C.; Roark, W. H.; Wilson, M.; Datta, K.; Guzman, R.; Han, H.-K.; Dyer, R. D. Discovery and characterization of a novel inhibitor of matrix metalloprotease-13 (MMP13) that reduces cartilage damage in vivo without joint fibroplasia side effects. *J. Biol. Chem.* **2007**, *282*, 27781–27791.

JM701274V